

**DETC2015-47610**

**PERFORMANCE COMPARISON OF A BULK THERMOELECTRIC COOLER WITH A  
HYBRID DEVICE ARCHITECTURE**

**Margaret Antonik**

Graduate Research Assistant  
North Carolina State University  
Raleigh, NC 27695, USA  
margaret\_antonik@ncsu.edu

**Scott M. Ferguson<sup>1</sup>**

Associate Professor  
North Carolina State University  
Raleigh, NC 27695, USA  
scott\_ferguson@ncsu.edu

**Brendan T. O'Connor**

Assistant Professor  
North Carolina State University  
Raleigh, NC 27695, USA  
brendan\_oconnor@ncsu.edu

**ABSTRACT**

This paper compares the economic viability and performance outcomes of two different thermoelectric device architectures to determine the advantages and appropriate use of each configuration. Hybrid thermoelectric coolers employ thin-film thermoelectric materials sandwiched between a plastic substrate and formed into a corrugated structure. Roll-to-roll manufacturing and low-cost polymer materials offer a cost advantage to the hybrid architecture at the sacrifice of performance capabilities while conventional bulk devices offer increased performance at a higher cost. Performance characteristics and cost information are developed for both hybrid and conventional bulk single-stage thermoelectric modules. The design variables include device geometry, electrical current input, and thermoelectric material type. The trade-offs between cooling performance and cost will be explored and the thermoelectric system configuration analyzed for both hybrid and conventional bulk thermoelectric coolers.

**NOMENCLATURE**

A Cross-sectional area  
C Cost  
C<sup>''</sup> Areal module cost  
C<sup>'''</sup> Volumetric module cost  
COP Coefficient of Performance  
d<sub>s</sub> Substrate thickness

I Input current  
K Thermal conductivity  
L TE leg length  
N Number of thermocouples  
P Input power  
Q Cooling/heating capacity  
R Electrical conductivity  
r Amortization rate  
T Absolute temperature  
t TE leg thickness  
U Heat exchanger overall heat transfer coefficient  
w TE leg width  
Z Thermoelectric material figure of merit

**Greek Symbols**

$\alpha$  Seebeck coefficient  
 $\kappa$  Thermal conductivity  
 $\rho$  Electrical resistivity  
 $\psi$  Dimensionless spreading resistance

<sup>1</sup>Corresponding author

## Subscripts

C	Cold side
H	Hot side
HX	Heat exchanger
n	n-type material
p	p-type material
s	substrate
TE	Thermoelectric material

## INTRODUCTION

Increased interest in sustainable practices and environmentally friendly products has driven the exploration of green technologies. Thermoelectric generators (TEGs) and coolers (TECs) offer the potential to be an important source of clean and renewable energy and an environmentally friendly way to heat and cool. Thermoelectric coolers might be a viable alternative to traditional vapor-compression refrigeration systems that employ potentially harmful refrigerants [1].

Thermoelectric (TE) devices are quiet, reliable, and scalable solid-state devices that use thermoelectric materials to 1) convert waste heat to energy via the Seebeck effect, or 2) convert energy to cooling or heating via the Peltier effect. A TE module is composed of thermocouples that consist of p-type and n-type TE elements. These elements are connected electrically in series and thermally in parallel and are sandwiched between an insulating substrate. Per the Peltier effect, a flow of current through the module produces a cooling effect on one side of the device [2]. If the current is reversed, a heating effect occurs.

The focus of this paper is on TECs as TEGs have been more widely explored for their performance limits and cost advantages. Additionally, design optimization and a better understanding of TEC characteristics may allow for expanded use in a variety of markets. Diverse applications of TECs include commercial products, military purposes, aerospace uses, scientific and medical equipment, microelectronics, and solar-driven thermoelectric cooling devices [3]. Climate-control seat systems constructed with TEC technology can reduce fuel consumption in hybrid vehicles [4]. TECs used in microprocessor cooling systems offer an efficient and cost-effective way of controlling chip temperatures [1], [4]. Solar-driven thermoelectric coolers and heaters are being investigated as heat pumps where the source of electrical power eliminates fossil power usage [5]. Historically, however, TE devices have not met the efficiency capabilities of current energy conversion or cooling technologies to reach widespread adoption.

TECs have the potential for widespread use, but a better understanding of the performance and design space is needed to drive future development. Despite recent advancements in the efficiency of the materials, additional improvements must be

weighed against the added overall system costs. Geometry of the device, power input into the cooler, operating parameters, and the heat exchanger characteristics are contributing factors to the efficiency of a TEC. Additionally, the exploration of different device architectures may allow for higher performing, lower cost TECs. This paper explores a hybrid architecture that combines a conventional bulk device with an in-plane thin film device. While taking advantage of low-cost roll-to-roll (R2R) manufacturing, the hybrid architecture is still able to maintain a cross-plane heat flux like that in a bulk device. Analysis is needed that goes beyond the scope of just studying thermoelectric materials and their efficiency to develop cost-effective, high performing TECs.

Toward this goal, this paper extends an existing cost-metric and expands the performance equations for a single-stage bulk TEC analysis. Additions include a heat exchanger and spreading resistance. Unlike previous analysis of TECs, this study considers two objectives, additional design variables and model considerations, a heat exchanger on the hot side of the TEC, and multiple TE materials. Furthermore, both bulk and hybrid device architectures are compared. Exploring the economic and performance characteristics of a TEC manufactured via screen-printing techniques offers insight into the viability of R2R manufacturing's applicability to TE devices.

A Nondominated-Sorting Genetic Algorithm-II (NSGA-II) is used to generate a set of Pareto efficient solutions that demonstrate the trade-offs between maximum cooling capacity per unit area ( $\text{W}/\text{m}^2$ ) and system cost per unit area ( $\$/\text{kWh}/\text{m}^2$ ) [6]. The cost metric, which includes both capital and manufacturing costs, will be explored in further detail to determine the major components of the total system costs, and trends in the design variables for the Pareto efficient solutions will be discussed. In considering these two objectives simultaneously, optimization of a single-stage TEC will be presented that accounts for the trade-offs between the comprehensive costs and performance of the system.

## BACKGROUND

In the 1990s, advances in the theory and concepts of electron and phonon transport in TE materials led to a renewed focus on thermoelectrics as a green technology [7]. Nanostructured and complex bulk materials allow for thermoelectric materials with improved efficiencies to compete with other technologies [8].  $ZT$ , given in Eq. (1), is the figure of merit measuring the efficiency of a thermoelectric material. A function of absolute temperature ( $T$ ), maximizing  $ZT$  requires a large Seebeck coefficient ( $\alpha$ ), low thermal conductivity ( $\kappa$ ), and low electrical resistivity ( $\rho$ ).

$$ZT = \frac{\alpha^2}{\kappa\rho} T \quad (1)$$

Typical  $ZT$  values of thermoelectric materials, including the widely used bismuth-telluride (BiTe) semiconductors, on the market are around 1 [4]. If average  $ZT$  values were greater than

2, thermoelectric heating, ventilating, and cooling systems could become attractive alternatives to traditional systems [4]. While presenting a trade-off in performance, low-cost and large-scale manufacturing of TE devices may provide an alternative to the conventional, difficult to manufacture bulk devices. Polymer TE materials, which are environmentally-friendly and stable, offer a printable solution that can be used in R2R manufacturing on flexible substrates. In comparison to current inorganic materials like BiTe, the best reported  $ZT$  value for polymer TE material poly(3,4-ethylenedioxythiophene) (PEDOT) is only 0.25 [9]. Ongoing research is exploring the screen printing of PEDOT in a R2R manufacturing process to produce thin-film TE devices.

Previous design and optimization research has focused on cooling capacity ( $Q_C$ ) and Coefficient of Performance ( $COP$ ), which measures the efficiency of a heat pump, with more recent analysis incorporating a cost metric. Yamanashi used dimensionless quantities to analyze the effects of the thermoelectric properties and heat exchangers and found that the hot side heat exchanger has greater effect on performance than the cold side heat exchanger [10]. Huang, Chin, and Duang used performance curves of actual TEC modules to analyze maximum  $COP$  and maximum  $Q_C$  designs [11]. Cheng and Lin used a genetic algorithm to maximize  $Q_C$  in a confined volume while treating  $COP$  and cost - calculated using TE material costs - as constraints [12]. Later work extended to multiobjective analysis of two-stage TECs [13].

Similarly, Nain et. al performed single and multiobjective analysis of TECs using a genetic algorithm and reported that the structural parameters of the TE elements (leg length and area) have significant influence on  $COP$  and  $Q_C$  [14]. Zhou and Yu maximized  $COP$  and  $Q_C$  separately by allocating thermal conductance of hot and cold heat exchangers [15]. Huang et. al used the simplified conjugate gradient method to optimize geometric structure for maximum  $Q_C$  with a constraint on  $COP$ , and found that leg length should be as small as possible with the area of the TE legs as large as possible [16]. Instead of using the aforementioned optimization methods, Venkata, Rao and Patel implemented a modified teaching-learning based optimization algorithm to maximize a weighted sum objective combining  $COP$  and  $Q_C$  for two-stage TECs [17]. Lastly, research by Khanh et. al tested the effectiveness of genetic algorithms and simulated annealing for single-stage TECs and indicated in a preliminary conclusion that simulated annealing was more robust [18].

Yazawa and Shakouri, Yee et. al, and LeBlanc et. al explored TECs and TEGs with a focus on the cost performance of the devices [19]–[21]. Yazawa and Shakouri explored the maximum power output of a TEG while considering the cost/efficiency trade-offs [19]. The heat exchanger and TEG were co-optimized to count total system performance, and inorganic and organic polymer materials were compared for optimization of power output per dollar ( $W/\$$ ) and mass of the device per unit of power ( $kg/W$ ). Their results indicated that polymer materials could prove advantageous in application. Yee et. al introduced a cost

per unit of power ( $W/\$$ ) cost metric (considering material, manufacturing, and heat exchanger costs) for TEGs, and optimized the TE leg length and system fill factor for the minimum  $W/\$$  [20]. While identifying regions of a performance space where different cost components dominated, the authors also concluded that very expensive TE materials can be cost effective in a TEG system if implemented with short TE legs and small fill factors. LeBlanc et. al extended the work of Yee et. al to include an analysis of more TE materials and to introduce a cost metric ( $\$/kWh$ ) for TECs [21]. These extensions provide the basis for the work completed in this paper. The next two sections will discuss the details of the TE model used and the modifications made to the cost metric for it to be incorporated in this application.

## MODELING OF SINGLE-STAGE TEC

### Device Architecture Types

Figure 1(a) shows a basic diagram of the architecture for a conventional, bulk TEC with a heat exchanger on one side and heat flowing through the device. The bulk architecture consists of p-type and n-type legs connected with metal contacts and then sandwiched between a substrate. In a similar manner, the architecture for the hybrid TEC maintains the cross-plane heat flux indicated in Fig. 1(a) while taking advantage of R2R processing. By maintaining the cross-plane heat flux, the hybrid device will be able to maintain more significant temperature differences across the TE legs unlike a thin-film device. The TE materials will be screen printed on a flexible plastic (PET) substrate in thicknesses between 50 and 250  $\mu m$  with a leg width over 10 mm and a leg length between 5 and 20 mm. Figure 1(b) depicts the printing pattern of the material on the PET substrate. After printing, the module is then processed to shape the device by maintaining the cross-plane heat flux like a bulk device by making the legs of the TEC perpendicular to a flat layer of PET substrate. It is supposed that the hybrid device will be suitable for applications requiring a very low heat flux over large areas.

### Fundamental Thermoelectric Modeling

A standard set of equations is widely used to model thermoelectric coolers [2]. As current is passed through the thermocouples, heat is absorbed at the cold side of the device and rejected at the hot side. Figure 1(a) depicts a generic thermal circuit model of a basic TEC. Another phenomenon present in TE devices is the Thomson effect, which describes the rate of generation of reversible heat across a device. The Thomson effect is neglected in this study as it has been shown that, for a wide range of temperatures, models incorporating the Thomson effect show close agreement with the standard set of TE equations not considering the effect [22]. For typical, commercially available TECs, the Thomson effect provides little improvement or degradation in  $Q_C$  and  $COP$  results.

Cooling using a TEC must overcome Joule heating (where the flow of electric current through the TE elements releases heat) and the heat conduction through the TEC legs (known as

the Fourier effect). Half of the Joule heating flows to each of the junctions of the TEC. Combining the Peltier effect, Joule heating, and the Fourier effect, the heat absorption into the device,  $Q_C$ , is given in Eq. (2). Similarly, the heat rejected at the hot side is given in Eq. (3). To simplify the analytical model, a heat sink is only considered on the hot side of the TEC. An infinite sink exists on the cold side, and the known ambient air temperature ( $T_\infty$ ) along with the heat exchanger heat transfer coefficient ( $U$ ) is used to determine the hot-side junction temperature ( $T_H$ ), calculated by Eq. (4). The heat conduction through the legs is between temperatures  $T_H$  and  $T_C$ .

$$Q_C = N \left[ I\alpha T_C - K(T_H - T_C) - \frac{1}{2} I^2 R \right] \quad (2)$$

$$Q_H = N \left[ I\alpha T_H - K(T_H - T_C) + \frac{1}{2} I^2 R \right] \quad (3)$$

$$T_H = Q_H \frac{1}{UA} + T_\infty \quad (4)$$

In these equations,  $N$  is the number of thermocouples,  $I$  is the input current,  $\alpha$  is the Seebeck coefficient,  $K$  is the thermal conductivity of the device, and  $R$  is the electrical resistivity.

The electrical power applied to the device needs to overcome the Seebeck voltage and the electrical resistance of the TE elements. The power input,  $P$  is shown in Eq. (5).

$$P = I\alpha(T_H - T_C) + I^2 R \quad (5)$$

The coefficient of performance, given in Eq. (6), expresses the efficiency of a TEC and is given by the heat absorbed by the device divided by the power expenditure into the device.

$$COP = \frac{Q_C}{P} \quad (6)$$

## Spreading Resistance

TE legs only occupy a fraction of the footprint of the substrate of the TEC, and the fill factors (ratio describing the area of the TE legs divided by area of the substrate) considered in the optimization problems for the bulk and hybrid devices range from small values nearing 0.01 to large values approaching 0.8. These fill factors influence the heat flow across the device; therefore, the thermal spreading resistance needs to be accounted for [19]. Widely used in electronics applications, a model developed by Song et. al is applied to TEC application as it allows for calculations for a rectangular geometry and has proven to be an accurate and simple approximation for spreading resistances [23].

To calculate spreading resistance, the first step is to convert the cross-sectional rectangular areas of the TE legs ( $A_{TE}$ ) and the device ( $A$ ) to circular geometries defined by radii  $a$  and  $b$ . This is given by Eq. (7) and (8). Using Eq. (9) and (10), dimensionless solutions for contact radius ( $\varepsilon$ ) and plate thickness ( $\tau$ ) are then determined. An empirical parameter ( $\lambda_c$ ), dimensionless parameter ( $\Phi_c$ ) and dimensionless constriction resistance ( $\psi$ ) used in the final equation for spreading resistance are calculated. These are given by Eq. (11)-(13). Finally, the spreading resistance ( $R_{spread}$ ) is determined by Eq. (14).

$$a = \sqrt{\frac{A_{TE}/2}{\pi}} \quad (7)$$

$$b = \sqrt{\frac{A/2}{\pi}} \quad (8)$$

$$\varepsilon = \frac{a}{b} \quad (9)$$

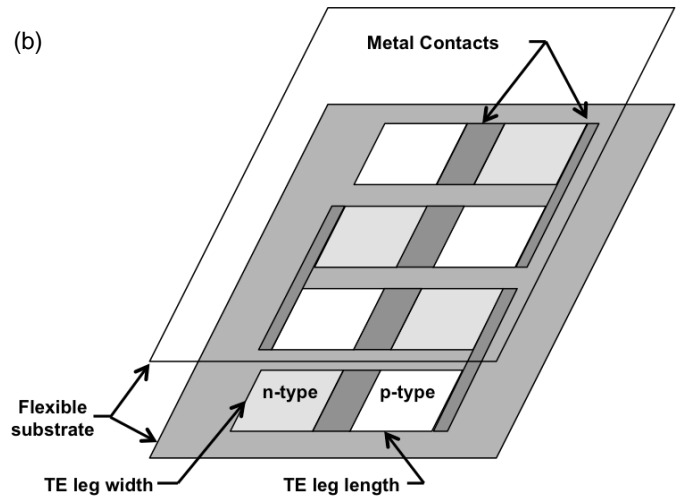
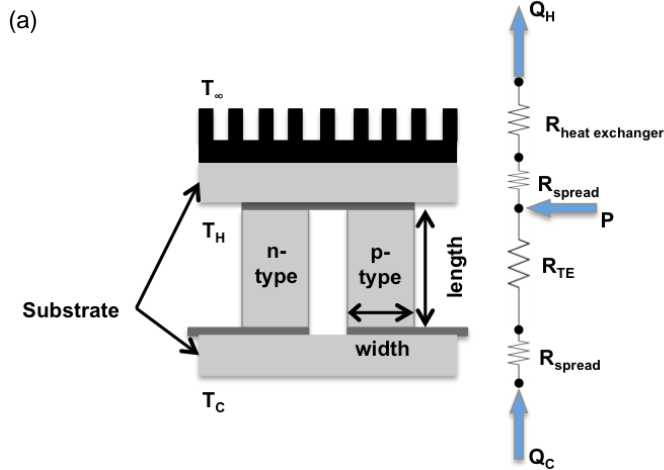


Figure 1. (a) Diagram of Basic TEC Architecture and Thermal Circuit Model and (b) Printing Pattern of Hybrid TE Device

$$\tau = \frac{d_s}{b} \quad (10)$$

$$\lambda_c = \pi + \frac{1}{\sqrt{\pi\varepsilon}} \quad (11)$$

$$\Phi_c = \frac{\tanh(\lambda_c \tau) + \frac{\lambda_c}{Bi}}{1 + \frac{\lambda_c}{Bi} \tanh(\lambda_c \tau)} \quad (12)$$

$$\psi = \frac{\varepsilon \tau}{\sqrt{\pi}} + 0.5(1 - \varepsilon)^{3/2} \Phi_c \quad (13)$$

$$R_{spread} = \frac{\psi}{\kappa_s \alpha \sqrt{\pi}} \quad (14)$$

In these equations,  $\kappa_s$  is the substrate thermal conductivity,  $d_s$  is the substrate thickness, and  $Bi$  is the Biot Number, which is ignored by the assumption that the temperature gradient inside the substrate is negligible.

### Material Properties

Additionally, the thermal resistance through the TE legs,  $R_{TE}$ , is given in Eq. (15). The total electrical resistance,  $R$ , thermal conductivity,  $K$ , and Seebeck coefficient,  $\alpha$ , are given in Eq. (16), (17), and (18).

$$R_{TE} = \frac{1}{(\kappa_p + \kappa_n) \frac{tW}{L}} \quad (15)$$

$$R = (\rho_p + \rho_n) \frac{L}{tW} \quad (16)$$

$$K = \frac{1}{R_{TE} + R_{spread}} \quad (17)$$

$$\alpha = \alpha_p + \alpha_n \quad (18)$$

In these equations,  $t$  is the thickness of the TE legs,  $w$  is the width, and  $L$  is the length of the legs.

Several common assumptions are made in the development of these basic equations. The p-type and n-type TE elements have the same basic geometries. The Seebeck coefficient, thermal conductivity, and electrical resistivity of the TE material are considered temperature independent. For simplicity, the thermal and electrical contact resistances of the substrate and the metal are treated as negligible, and as stated previously, the Thomson effect is also neglected. The same set of equations is used to evaluate the performance metrics for both the hybrid and bulk architectures. The overarching structure of the devices remains the same, but the geometries (e.g. leg thickness, width, and length) are altered to reflect the different architecture. While this is a simplification, it allows for a first pass comparison of the advantages and disadvantages of the architectures.

### DEVICE COST METRIC

The breakdown of the cost of a TEC and the parameters that contribute to the cost are given in Figure 2. The cost metric analysis is derived from [20] and [21]. While [20] and [21]

consider heat exchangers in their cost metric for TEGs, a contribution of this work is to also incorporate heat exchangers into the analysis of a TEC. To consider the effect of the heat exchanger on the design of a TEC as well as the substrate properties, Yee et. al's equation for the capital cost of a TEC is divided into heat exchanger and substrate cost. This also allows for the quick use of this cost metric in multiple device architectures and for varying substrate materials.

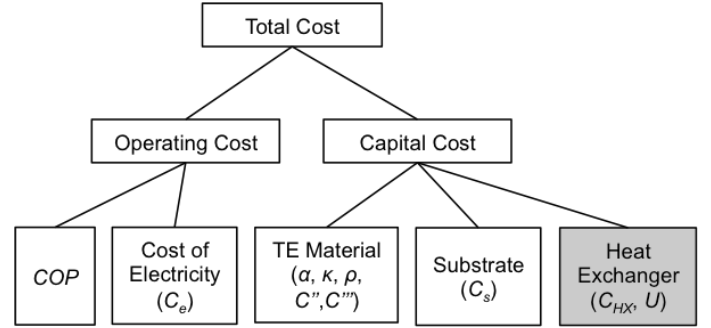


Figure 2. Breakdown of Total System Cost

Device geometry and material, manufacturing, and heat exchanger costs are considered key components in a cost metric for a TE device [20],[21]. Yee et. al, present a cost metric that includes these components while incorporating volumetric module costs,  $C'''$ , areal module costs,  $C''$ , and heat exchanger costs (including the ceramic substrate),  $C_{HX}$  [20]. This metric is also used by LeBlanc et. al, but the heat exchanger component is ignored for TECs [21]. To analyze the total system cost of a TEC and to study the bulk and hybrid architectures, the heat exchanger/substrate component of Yee et. al's cost metric is separated into heat exchanger cost and then substrate cost,  $C_s$ . Using the volumetric, areal, heat exchanger, and substrate cost components, the overall system cost,  $C$ , of a TEC is given in Eq. (19).

$$C = N[(C'''L + C'')wt + C_{HX}UA + C_sA] \quad (19)$$

The manufacturing costs gathered by LeBlanc et. al are an appropriate lower bound for the estimated costs of manufacturing a TEC [21], [24]. The volumetric module costs include the cost of the thermoelectric material, volumetric manufacturing costs like ball milling and hot pressing, and any other costs associated with the volumetric amount of thermoelectric material. Likewise, the areal module costs include the cost of metallization, areal manufacturing costs such as dicing and cutting, and other costs that scale with the area of the device. Material cost was gathered from raw material costs reported in the *U.S. Geological Survey*. Heat exchanger costs were derived from data in Shah and Sekulic's work on heat exchanger design and are closely related to the heat transfer coefficient of the exchanger as more complex designs increase the cost of the exchanger [25], [26].

LeBlanc et. al incorporated an operating cost of the TEC to consider the efficiency of the device in addition to the capital cost [21]. With this cost metric,  $COP$  is considered to calculate

an operating cost with continuous operation over a 20-year period (the industry standard for the mean time between failures is over 200,000 hours). This cost metric, given in Eq. (20) is expressed in \$/kWh and includes the capital cost amortized over the lifetime and the lifetime operating cost.

$$H = \frac{C_e}{COP} + r \frac{C}{COP \cdot P} \quad (20)$$

$C_e$  is the price of electricity and  $r$  is the amortization rate.

By dividing Yee et. al's overall system cost into TE elements, heat exchanger, and substrate costs, both traditional methods of manufacturing and screen-printing techniques can be analyzed. Additionally, LeBlanc et. al did not include heat exchangers in their analysis of TECs but found that the heat exchanger is a large component of the cost of TEGs. The heat exchanger can also greatly impact the performance characteristics of a TEC. Consequently, the cost metric and TEC model used in the literature was modified to include heat exchangers, allow for different device geometries, and incorporate additional substrate materials.

The same TE materials analyzed by LeBlanc et. al for conventional bulk devices are used in this analysis. A BiTe-polymer composite printable material introduced by Chen et. al is introduced to the optimization for printable, hybrid TECs, and PEDOT material properties are updated to reflect the results from Bubnova et. al [9][27]. To use BiTe as a printable solution, which has only recently been the focus of extended research, BiTe is mixed with polymer binders and solvents. The result is a composite TE material with a  $ZT$  value of 0.18. These materials and their TE properties and cost are given in the appendix.

## DESIGN OPTIMIZATION

In engineering design optimization, the objective is to find the design parameters that result in the optimal set of performance goals. Multiobjective optimization strives to equip designers with the information needed to make timely, knowledge-based decisions. With multiple objectives, the solution to an optimization problem is no longer a single point, as trade-offs between the different objectives may exist. A nondominated design point is known as a Pareto efficient solution, meaning the solution cannot be improved with respect to one objective without worsening at least one other objective. The Pareto set is an entire set of nondominated design points [28]. In this paper, NSGA-II is used to find the optimum set of nondominated design points.

## Problem Formulation

The goal of the optimization problem is to determine the optimal device parameters to maximize cooling capacity ( $Q_C$ ) per area (heat flux) of the TEC and minimize the total device cost ( $H$ ) per area. These objectives are defined instead of studying  $Q_C$  and  $H$  so the bulk and hybrid architectures can be compared. The hybrid device is thought be advantageous for low-density cooling, large area applications while offering cost

competitiveness to the bulk device. Without information on the differences in cooling output of a hybrid and a bulk device to confine the area in the optimization problem, maximizing  $Q_C$  and minimizing  $H$  would not allow for a comparison of the architectures. By comparing the heat flux and cost per area for similar sized devices, the advantages and disadvantages of the different architectures can more readily be deduced.

For the purpose of this study, the operating temperatures are set at an ambient temperature of 20°C with the cold-side temperature at 0°C. Alumina ceramic is the substrate for the bulk device, and PET plastic is the substrate for the hybrid architecture. Table 1 details the device properties and operating parameters used in this analysis to model the bulk and hybrid TECs and the cost metric.

**Table 1. Device Properties and Operating Parameters Used in Analysis**

Property	Value	Ref.
$T_\infty$	20°C	-
$T_C$	0°C	-
$C''_{bulk}$	\$168.23/m <sup>2</sup>	[21]
$C''_{hybrid}$	\$4.76/m <sup>2</sup>	[21]
$C_{HX}$	\$7.60/(W/K)	[21]
$C_e$	\$0.1035/kWh	[29]
$C_{s,bulk}$	\$0.8625/m <sup>2</sup>	[25]
$C_{s,hybrid}$	\$0.3985/m <sup>2</sup>	[30]
$C_{HX}$	\$7.60/(W/K)	[21]
$d_{s,bulk}$	0.5 mm	-
$d_{s,hybrid}$	125 μm	-
$k_{s,bulk}$	30 W m <sup>-1</sup> K <sup>-1</sup>	[31]
$k_{s,hybrid}$	0.15 W m <sup>-1</sup> K <sup>-1</sup>	[32]
$r$	3% annually	[21]
$U$	100 W m <sup>-2</sup> K <sup>-1</sup>	[20]

The design variables considered are the thickness of the TE leg ( $t$ ), width of the TE leg ( $w$ ), length of the TE leg ( $L$ ), the space between the legs ( $\delta$ ), input current ( $I$ ), p-type material, n-type material, and the number of thermocouples. Bounds for the optimization algorithm of a bulk TEC are set by manufacturing constraints and those established in the literature. Twenty-five different material choices, and their associated cost, Seebeck coefficient, thermal conductivity, and electrical resistivity, were investigated for the bulk optimization problem. The problem statement is given by Eq. (21).

$$\begin{aligned}
\text{Minimize: } & F_1: H/A \text{ [$/kWh per m}^2\text{]} & (21) \\
& F_2: -Q_c/A \text{ [W/m}^2\text{]} \\
\text{Subject to: } & 0.5 \text{ mm} \leq t \leq 0.8 \text{ mm} \\
& 0.5 \text{ mm} \leq w \leq 0.8 \text{ mm} \\
& 0.1 \text{ mm} \leq L \leq 1 \text{ mm} \\
& 0.1 \text{ mm} \leq \delta \leq 4 \text{ mm} \\
& 0.1 \text{ A} \leq I \leq 5 \text{ A} \\
& 1 \leq \text{material}_{n\text{-type}} \leq 25 \\
& \quad \text{where } \text{material}_{n\text{-type}} \in \mathbb{Z} \\
& 1 \leq \text{material}_{p\text{-type}} \leq 25 \\
& \quad \text{where } \text{material}_{p\text{-type}} \in \mathbb{Z} \\
& 1 \leq N \leq 200 \text{ for } N \in \mathbb{Z}
\end{aligned}$$

The structure of the formulated problem for the hybrid architecture is identical to that of the bulk architecture, but the bounds are changed to reflect the changes in geometry of the TEC. Additional manufacturing considerations for screen-printed inks and processing of the PET substrate are also considered when setting the bounds on the design variables. Two different material choices, and their associated cost, Seebeck coefficient, thermal conductivity, and electrical resistivity, were available for the hybrid optimization problem. The formal problem statement is given in Eq. (22).

$$\begin{aligned}
\text{Minimize: } & F_1: H/A \text{ [$/kWh per m}^2\text{]} & (22) \\
& F_2: -Q_c/A \text{ [W/m}^2\text{]} \\
\text{Subject to: } & 50 \text{ }\mu\text{m} \leq t \leq 250 \text{ }\mu\text{m} \\
& 10 \text{ mm} \leq w \leq 20 \text{ mm} \\
& 5 \text{ mm} \leq L \leq 20 \text{ mm} \\
& 0.1 \text{ mm} \leq \delta \leq 4 \text{ mm} \\
& 0.1 \text{ A} \leq I \leq 10 \text{ A}
\end{aligned}$$

$$\begin{aligned}
1 \leq \text{material}_{n\text{-type}} \leq 2 & & (22) \\
\text{where } \text{material}_{n\text{-type}} \in \mathbb{Z} \\
1 \leq \text{material}_{p\text{-type}} \leq 2 \\
\text{where } \text{material}_{p\text{-type}} \in \mathbb{Z} \\
1 \leq N \leq 200 \text{ for } N \in \mathbb{Z}
\end{aligned}$$

As a population-based approach, NSGA-II is well suited to this multiobjective problem [6]. The algorithm is robust and is able to explore the objective space for a diverse set of solutions in a complex problem. For this study, the size of the population at each generation was set to 80 designs, 10 times the number of design variables. The selection method was tournament with 4 candidates, and the crossover operator is scattered with 0.5 crossover rate. The mutation operator is uniform with a 5% chance of mutation. The algorithm terminated after 100 generations, and a measure of hypervolume was calculated to ensure the algorithm had converged. As discussed further, all evaluated points and their corresponding function values from the optimization algorithm are used in developing the set of Pareto efficient solutions.

## RESULTS

Pareto frontiers were generated according to the problem statements given in Eq. (21) and (22). The Pareto efficient solutions are shown in Figure 3(a) for the bulk and hybrid devices. As context, ongoing research is exploring the use of TECs in high heat flux ( $>100,000 \text{ W/m}^2$ ) applications like actively cooling electronic devices, but current designs have  $COPs$  less than 1 (operating cost calculated by  $C_e$  divided by  $COP$  would be greater than  $\$0.1035/\text{kWh}$ ) [33]. The heat flux of R134a direct expansion evaporator coils used in air conditioning and refrigeration can range from  $6000\text{-}8500 \text{ W/m}^2$ , and an Energy Star rated central air conditioning unit must have a  $COP$  greater than 3.22, which translates to an operating cost of  $\$0.0321/\text{kWh}$  [34].

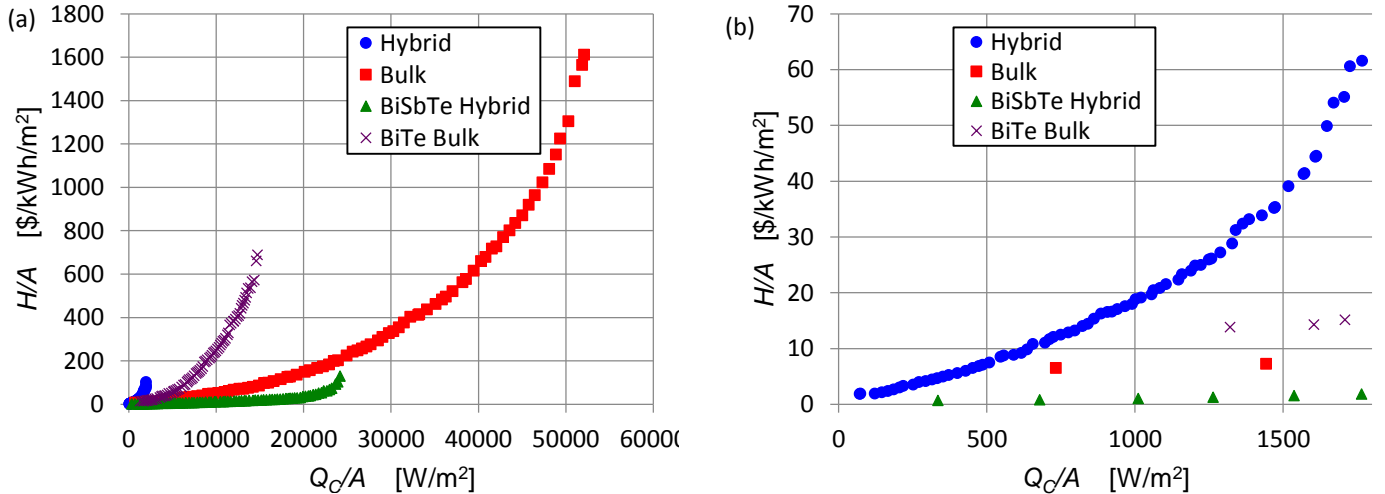


Figure 3. (a) Pareto Frontiers and (b) Magnified Pareto Frontiers

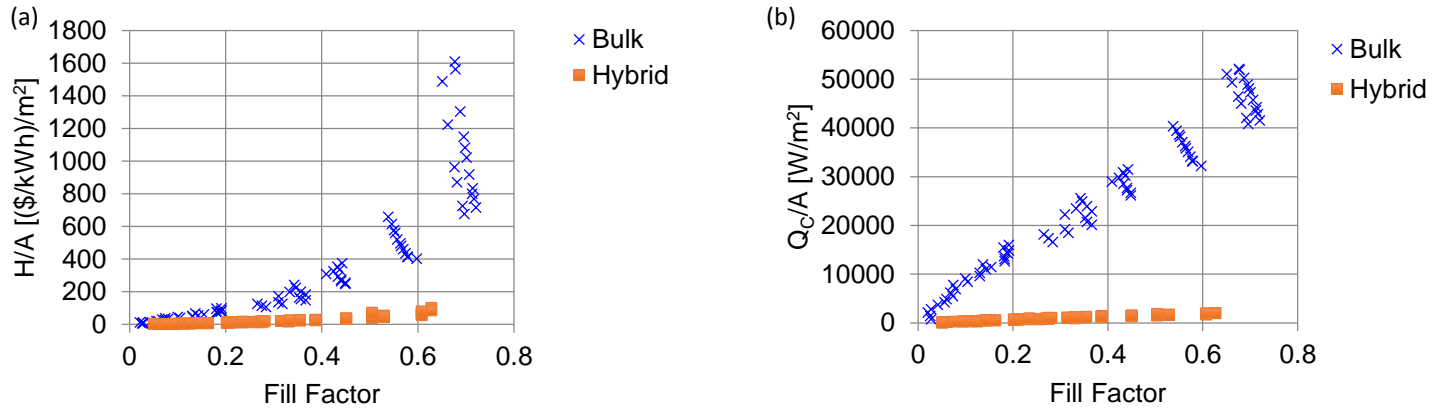


Figure 4. (a) Fill Factor versus  $H/A$  and (b) Fill Factor versus  $Q_c/A$

Every efficient design populating the frontier from the hybrid architecture had the polymer (PEDOT) material choice, and every efficient design from the bulk architecture optimization used the BiSbTe nanobulk material. This is analogous to the results seen in LeBlanc et. al's study where the BiSbTe nanobulk material (identified as having nanoscale grain structures) performs well on a \$/kWh basis [21]. Also, given in Figure 3 is a Pareto frontier for bulk devices when the n-type and p-type material type is limited to the commonly used BiTe. Printable TE materials that are currently available for application are limiting the performance of the hybrid device. To identify the potential of the hybrid architecture if printable technologies improved in efficiency, a frontier limiting the material choice to BiSbTe nanobulk for a hybrid device is shown in Figure 3..

A Pareto frontier for the case limiting the material choice to the commonly used BiTe semiconductor but maintaining the bounds on the other design variables provides a baseline for measuring performance improvements. By including the TE material type as a design variable, significant performance improvements are seen at high heat fluxes. The polymer hybrid device performs poorly in both objectives when compared to the alternative bulk devices. Figure 3(b) magnifies the Pareto frontier results given in Figure 3(a). Even at low cooling density applications, the cost performance of the polymer hybrid device does not improve over the bulk devices. For example, at approximately 1300 W/m<sup>2</sup>, a BiTe bulk device is more

economically attractive than the polymer hybrid. Also to note, the median COP of the polymer hybrid Pareto efficient solutions was 0.83 with the median COP of the bulk solutions similar at 0.79.

As previously mentioned, the highest reported  $ZT$  value for polymer materials is 0.25. The BiSbTe nanobulk material used in this study has a  $ZT$  of approximately 1.6. If a material this efficient were available as a printable solution, the hybrid device would be capable of higher heat flux applications at a lower cost than the bulk device with the same material. However, a region of the performance space at very large heat fluxes (>27,000 W/m<sup>2</sup>) remains infeasible for the BiSbTe hybrid device.

Typically, the heat flux of a device is increased by decreasing the leg length of the TEC and increasing the area of the legs, but manufacturing constraints on the hybrid device limit the ratio of the leg area to length. According to manufacturer data, the thickest a solution can be deposited with a rotary screen printer is 250  $\mu\text{m}$ , and the leg length's lower bound is constrained by how the flexible substrate can be processed into a form that mimics the cross-plane heat flux of a bulk TEC. Additionally, hybrid devices have limited the material selection choices as printable solutions are needed for R2R manufacturing. The design variables of the Pareto efficient solutions reflect this, as the leg thickness and width is pushed to the upper bounds and the length of the legs is pushed to the lower bound. The primary difference between the two extreme values

Table 2. Design Variable Values at Extreme Pareto Efficient Solutions

Device Architecture	Objective	Objective Values at Extreme	Design Variable							
			$t$ (mm)	$w$ (mm)	$L$ (mm)	$\delta$ (mm)	$I$ (A)	$material_n$	$material_p$	$N$
Bulk	Minimum H/A	\$6.48/kWh/m <sup>2</sup> 732.7 W/m <sup>2</sup>	0.80	0.78	1.00	3.94	0.58	BiSbTe	BiSbTe	200
	Maximum Qc/A	52092 W/m <sup>2</sup> \$1611/kWh/m <sup>2</sup>	0.51	0.50	1.00	0.11	0.91	BiSbTe	BiSbTe	200
Hybrid	Minimum H/A	\$1.81 \$/kWh/m <sup>2</sup> 70.8 W/m <sup>2</sup>	0.25	19.96	5.00	3.80	0.15	PEDOT	PEDOT	199
	Maximum Qc/A	1989.7 W/m <sup>2</sup> \$101.67/kWh/m <sup>2</sup>	0.25	19.96	5.07	0.15	0.82	PEDOT	PEDOT	199

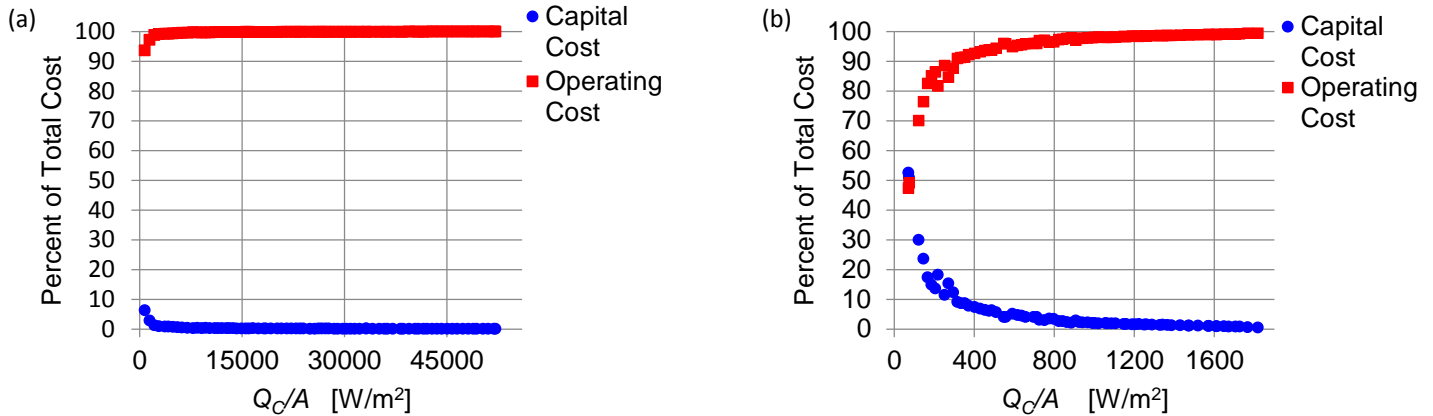


Figure 5. (a) Cost Breakdown of Bulk Device and (b) Hybrid Device

is the spacing between the TE legs. By spreading out the thermocouples and thus decreasing the fill factor, the cost of the module is lower, but cooling capacity is compromised. Table 2 provides values of the extreme solutions in the frontiers for the hybrid and bulk devices and the design variables that produce the objective values, and Figure 4 shows fill factor versus cost and fill factor versus cooling capacity of the bulk and hybrid devices that demonstrate the trade-off between cost and cooling capacity performance.

To further investigate the cost metric, total cost is broken down into operating and capital costs. Figures 5(a) and 5(b) provide a breakdown of the total cost for both device architectures as a percentage of total cost. The operating cost of both the bulk and the hybrid makes up a majority of the total system cost of a TEC, so consideration of the device efficiency is paramount. The capital cost is also amortized over a 20 year lifetime so this lends to how the operating cost dominates.

When investigating the capital cost of the TEC, it is observed that the heat exchanger is a large component of the system capital cost. The heat exchanger cost for the Pareto efficient solutions of the bulk TEC accounts for 68.3% on average of the total capital cost. Volumetric material cost contributes 26.5%, and areal material cost contributes 0.5%. For the hybrid device, the heat exchanger cost comprises 99.7% on average of the total capital cost with volumetric material cost contributing 0.01% and areal cost approximately 0.02%. For both architectures, the substrate cost is a very small percentage.

## CONCLUSIONS

When selecting a TEC module, three parameters are generally needed to select a design: required cooling capacity, cold side temperature, and hot side temperature. While it is common throughout the literature to study optimal TECs and consider these three specifications, this study attempts to work towards real world applications by incorporating a cost metric and considering multiple facets of a TEC system, including heat exchangers and spreading resistance. Design optimization aimed at improving the performance of a TEC and a better

understanding of TEC characteristics may allow for expanded use of TECs in a variety of markets. While previous design research on TECs has focused only on certain aspects, this study adds to the overall body of research on TECs and works towards realizing real world applications through the consideration of system cost. The goal is to bridge the gap between theoretical aspects of TECs and actual design considerations.

This paper extends the work of other researchers by considering the multiobjective optimization of two different TEC architectures. To facilitate this optimization, the cost metric identified by Yee et. al is modified to accommodate the hybrid architecture [20]. Optimization results allow for comparisons between architectures while ensuring that the designs are evaluated for maximum cooling capacity and minimum cost. Like previous research, this analysis showed that maximizing leg area while decreasing leg length results in increased cooling capacities. Additionally, the BiSbTe nanobulk TE material is a promising alternative to the conventional BiTe modules currently on the market.

Results of the multiobjective optimization demonstrated the trade-off between cost and device performance. At different regions of the performance space, one device architecture or material choice may be a more appropriate solution for a given application. At high heat flux requirements, the bulk device with BiSbTe nanobulk TE material is the only option, but at lower heat flux requirements, both the hybrid and bulk devices are an option. However, the analysis suggests that the bulk device may still be the more economical alternative. After comparing results, it is evident that even in low cooling density applications, the hybrid device architecture is not economically viable when compared to a bulk device. If printable TE materials can be improved to  $ZT$  values similar to the material choices available for bulk devices, the hybrid architecture becomes a more attractive solution as its cost per area is less for a given heat flux than the bulk device.

Additionally, a majority of the total cost of a device is associated to operating cost, so consideration of the material efficiency and device COP is integral in the design of a TEC.

These trends are similar in both the hybrid and bulk architectures. Capital cost, however, is still an important factor in designing a TEC. Heat exchangers are the largest component of the TEC capital cost, especially with the hybrid device architecture. The material cost is more expensive for the bulk devices, but the inexpensive polymer hybrid device is unable to compete from a performance standpoint with bulk devices and the materials with higher  $ZT$  values.

Future work includes an analysis of additional device architectures, including thin-film devices and a hybrid architecture with a sinusoidal structure. It is evident that manufacturing constraints are limiting the performance of both the bulk and hybrid devices and that the cost of the heat exchangers is a prohibiting factor in the capital cost. While advancements in materials and manufacturing techniques are outside the scope of this research, further exploration of the limitations placed on the device architectures by currently available technology and of the available options for heat exchanger optimization is warranted. A detailed cost metric that comprehensively models the R2R manufacturing process for hybrid devices and the production of bulk TECs could contribute to a better understanding of these limitations. In addition, both R2R processing and device prototypes would provide a better understanding of the cost and cooling performance of the device architectures.

## ACKNOWLEDGMENTS

We gratefully acknowledge support from Eastman Chemical. Any opinions, findings, and conclusions presented in this paper are those of the authors and do not necessarily reflect the views of Eastman Chemical.

## REFERENCES

- [1] F. J. DiSalvo, "Thermoelectric Cooling and Power Generation," *Science*, vol. 285, no. 5428, pp. 703–706, Jul. 1999.
- [2] D. M. Rowe, *Thermoelectrics handbook [electronic resource]: macro to nano*. Boca Raton: CRC/Taylor & Francis, 2006.
- [3] Ferrotec, "Thermal Reference Guide," *Ferrotec*. [Online]. Available: <https://thermal.ferrotec.com/technology/thermal/thermoelctric-reference-guide/>. [Accessed: 26-Jan-2014].
- [4] L. E. Bell, "Cooling, Heating, Generating Power, and Recovering Waste Heat with Thermoelectric Systems," *Science*, vol. 321, no. 5895, pp. 1457–1461, Sep. 2008.
- [5] T.-C. Cheng, C.-H. Cheng, Z.-Z. Huang, and G.-C. Liao, "Development of an energy-saving module via combination of solar cells and thermoelectric coolers for green building applications," *Energy*, vol. 36, no. 1, pp. 133–140, Jan. 2011.
- [6] K. Deb, A. Pratap, S. Agarwal, and T. Meyarivan, "A fast and elitist multiobjective genetic algorithm: NSGA-II," *IEEE Trans. Evol. Comput.*, vol. 6, no. 2, pp. 182–197, Apr. 2002.
- [7] G. Chen, M. S. Dresselhaus, G. Dresselhaus, J.-P. Fleurial, and T. Caillat, "Recent developments in thermoelectric materials," *Int. Mater. Rev.*, vol. 48, no. 1, pp. 45–66, Feb. 2003.
- [8] G. J. Snyder and E. S. Toberer, "Complex thermoelectric materials," *Nat. Mater.*, vol. 7, no. 2, pp. 105–114, Feb. 2008.
- [9] O. Bubnova, Z. U. Khan, A. Malti, S. Braun, M. Fahlman, M. Berggren, and X. Crispin, "Optimization of the thermoelectric figure of merit in the conducting polymer poly(3,4-ethylenedioxythiophene)," *Nat. Mater.*, vol. 10, no. 6, pp. 429–433, Jun. 2011.
- [10] M. Yamanashi, "A new approach to optimum design in thermoelectric cooling systems," *J. Appl. Phys.*, vol. 80, no. 9, pp. 5494–5502, Nov. 1996.
- [11] B. J. Huang, C. J. Chin, and C. L. Duang, "A design method of thermoelectric cooler," *Int. J. Refrig.*, vol. 23, no. 3, pp. 208–218, May 2000.
- [12] Y.-H. Cheng and W.-K. Lin, "Geometric optimization of thermoelectric coolers in a confined volume using genetic algorithms," *Appl. Therm. Eng.*, vol. 25, no. 17–18, pp. 2983–2997, Dec. 2005.
- [13] Y.-H. Cheng and C. Shih, "Maximizing the cooling capacity and COP of two-stage thermoelectric coolers through genetic algorithm," *Appl. Therm. Eng.*, vol. 26, no. 8–9, pp. 937–947, Jun. 2006.
- [14] P. K. S. Nain, J. M. Giri, S. Sharma, and K. Deb, "Multi-objective Performance Optimization of Thermo-Electric Coolers Using Dimensional Structural Parameters," in *Swarm, Evolutionary, and Memetic Computing*, vol. 6466, B. K. Panigrahi, S. Das, P. N. Suganthan, and S. S. Dash, Eds. Berlin: Springer-Verlag Berlin, 2010, pp. 607–614.
- [15] Y. Zhou and J. Yu, "Design optimization of thermoelectric cooling systems for applications in electronic devices," *Int. J. Refrig.-Rev. Int. Froid*, vol. 35, no. 4, pp. 1139–1144, Jun. 2012.
- [16] Y.-X. Huang, X.-D. Wang, C.-H. Cheng, and D. T.-W. Lin, "Geometry optimization of thermoelectric coolers using simplified conjugate-gradient method," *Energy*, vol. 59, pp. 689–697, Sep. 2013.
- [17] R. Venkata Rao and V. Patel, "Multi-objective optimization of two stage thermoelectric cooler using a modified teaching–learning-based optimization algorithm," *Eng. Appl. Artif. Intell.*, vol. 26, no. 1, pp. 430–445, Jan. 2013.
- [18] D. V. K. Khanh, P. Vasant, I. Elamvazuthi, and V. N. Dieu, "Optimization Of Thermo-Electric Coolers Using Hybrid Genetic Algorithm And Simulated Annealing," *Arch. Control Sci.*, vol. 24, no. 2, pp. 155–176, 2014.
- [19] K. Yazawa and A. Shakouri, "Scalable Cost/Performance Analysis for Thermoelectric Waste Heat Recovery Systems," *J. Electron. Mater.*, Jun. 2012.
- [20] S. K. Yee, S. LeBlanc, K. E. Goodson, and C. Dames, "\$ per W metrics for thermoelectric power generation: beyond  $ZT$ ," *Energy Environ. Sci.*, vol. 6, no. 9, pp. 2561–2571, Aug. 2013.

[21] S. LeBlanc, S. K. Yee, M. L. Scullin, C. Dames, and K. E. Goodson, "Material and manufacturing cost considerations for thermoelectrics," *Renew. Sustain. Energy Rev.*, vol. 32, pp. 313–327, Apr. 2014.

[22] H. Lee, "The Thomson effect and the ideal equation on thermoelectric coolers," *Energy*, vol. 56, pp. 61–69, Jul. 2013.

[23] S. Song, V. Au, and K. P. Moran, "Constriction/spreading resistance model for electronics packaging," in *Proceedings of the 4th ASME/JSME thermal engineering joint conference*, 1995, vol. 4, pp. 199–206.

[24] L. M. Matthews, *Estimating manufacturing costs: a practical guide for managers and estimators* /. McGraw-Hill, c1983.

[25] "National Minerals Information Center," *Minerals Statistics and Information from the USGS*. .

[26] R. K. Shah and D. P. Sekulic, *Fundamentals of Heat Exchanger Design*. John Wiley & Sons, 2003.

[27] A. Chen, D. Madan, P. K. Wright, and J. W. Evans, "Dispenser-printed planar thick-film thermoelectric energy generators," *J. Micromechanics Microengineering*, vol. 21, no. 10, p. 104006, Oct. 2011.

[28] V. Pareto, *Manual of political economy*. New York: A. M. Kelley, 1971.

[29] R. Hankey, C. Cassar, R. Peterson, P. Wong, and J. Knaub, Jr., "Electric Power Monthly with Data for October 2014," U.S. Department of Energy, Washington, DC, Dec. 2014.

[30] F. Esposito, "Resin Pricing," *Plastics News*, 12-Jan-2015. [Online]. Available: <http://www.plasticsnews.com/resin/engineering-thermoplastics/current-pricing>.

[31] P. Auerkari, "Mechanical and physical properties of engineering alumina ceramics," 1996.

[32] J. Speight, *Lange's Handbook of Chemistry, 70th Anniversary Edition*. McGraw-Hill Companies, Incorporated, 2004.

[33] R. Ranjan, J. E. Turney, C. E. Lents, and V. H. Faustino, "Design of Thermoelectric Modules for High Heat Flux Cooling," *J. Electron. Packag.*, vol. 136, no. 4, p. 041001, Dec. 2014.

[34] "Air-Source Heat Pumps and Central Air Conditioners Key Product Criteria," *Energy Star*, 19-Jan-2015. [Online]. Available: <https://www.energystar.gov>.

## APPENDIX

### Bulk Material Selection

Material	Type	$\alpha$ (V/K)	$\rho$ ( $\Omega$ mm)	$\kappa$ (W/mm-K)	$C'''$ (\$/mm <sup>3</sup> )	$C''$ (\$/mm <sup>2</sup> )	Ref.
Bi <sub>2</sub> Te <sub>3</sub>	Bulk	-0.000227	0.011474864	0.00157	0.000889565	0.00016823	[21]
Bi <sub>0.52</sub> Sb <sub>1.48</sub> Te <sub>3</sub>	Bulk	0.000202	0.007702973	0.00141	0.000865743	0.00016823	[21]
AgPb <sub>18</sub> SbTe <sub>20</sub>	Bulk	-0.000121	0.005076142	0.00228	0.00077717	0.00016823	[21]
SiGe	Bulk	0.000117	0.01075963	0.00495	0.003044917	0.00016823	[21]
Mg <sub>2</sub> Si <sub>0.6</sub> Sn <sub>0.4</sub>	Bulk	-0.000089	0.00513901	0.0033	1.68306E-05	0.00016823	[21]
MnSi <sub>1.75</sub>	Bulk	0.000183	0.127129418	0.00234	7.33212E-06	0.00016823	[21]
Ba <sub>8</sub> Ga <sub>16</sub> Ge <sub>28</sub> Zn <sub>2</sub>	Bulk	-0.00011	0.033696128	0.00139	0.003123358	0.00016823	[21]
Ba <sub>8</sub> Ga <sub>16</sub> Ge <sub>30</sub>	Bulk	-0.000035	0.006281802	0.00172	0.003230061	0.00016823	[21]
Ba <sub>7</sub> Sr <sub>1</sub> Al <sub>16</sub> Si <sub>30</sub>	Bulk	-0.000023	0.00569833	0.00237	0.000005346	0.00016823	[21]
CeFe <sub>4</sub> Sb <sub>12</sub>	Bulk	0.000074	0.004444642	0.0026	0.000262299	0.00016823	[21]
Yb <sub>0.2</sub> In <sub>0.2</sub> Co <sub>4</sub> Sb <sub>12</sub>	Bulk	-0.00013	0.006144016	0.00325	0.000193688	0.00016823	[21]
Ca <sub>0.18</sub> Co <sub>3.97</sub> Ni <sub>0.03</sub> Sb <sub>12.40</sub>	Bulk	-0.000124	0.005062778	0.00571	9.3016E-05	0.00016823	[21]
(Zn <sub>0.98</sub> Al <sub>0.02</sub> )O	Bulk	-0.000084	0.01173282	0.04073	0.000020128	0.00016823	[21]
Ca <sub>2.4</sub> Bi <sub>0.3</sub> Na <sub>0.3</sub> Co <sub>4</sub> O <sub>9</sub>	Bulk	0.000124	0.093826234	0.00201	0.00017294	0.00016823	[21]
Na <sub>0.7</sub> CoO <sub>2.8</sub>	Bulk	0.000081	0.003024529	0.01993	0.000195925	0.00016823	[21]
Zr <sub>0.25</sub> Hf <sub>0.25</sub> Ti <sub>0.5</sub> NiSn <sub>0.994</sub> Sb <sub>0.006</sub>	Bulk	-0.000208	0.012187988	0.00286	8.06371E-05	0.00016823	[21]
Zr <sub>0.5</sub> Hf <sub>0.5</sub> Ni <sub>0.8</sub> Pd <sub>0.2</sub> Sn <sub>0.99</sub> Sb <sub>0.01</sub>	Bulk	-0.000103	0.004784689	0.00464	9.1203E-05	0.00016823	[21]
Ti <sub>0.8</sub> Hf <sub>0.2</sub> NiSn	Bulk	-0.000115	0.042971939	0.00405	8.64239E-05	0.00016823	[21]
Bi <sub>0.52</sub> Sb <sub>1.48</sub> Te <sub>3</sub>	Nanobulk	0.000224	0.013176967	0.00068	0.00087975	0.00016823	[21]
(Na <sub>0.0283</sub> Pb <sub>0.945</sub> Te <sub>0.9733</sub> )(Ag <sub>1.11</sub> Te <sub>0.555</sub> )	Nanobulk	0.000069	0.01140576	0.00171	0.000748177	0.00016823	[21]
Si <sub>80</sub> Ge <sub>20</sub>	Nanobulk	0.000114	0.011866619	0.00246	0.001303838	0.00016823	[21]
Mg <sub>2</sub> Si <sub>0.85</sub> Bi <sub>0.15</sub>	Nanobulk	0.000098	0.008305648	0.00752	3.34809E-05	0.00016823	[21]
Si	Nanobulk	-0.000064	0.004816492	0.0128	9.7627E-06	0.00016823	[21]
Mn <sub>15</sub> Si <sub>28</sub>	Nanobulk	0.000111	0.029804483	0.00275	1.09881E-05	0.00016823	[21]
PEDOT:PSS	Polymer	0.00021	0.135135135	0.00037	0.00000051	0.00000476	[9]

### Hybrid Material Selection

Material	Type	$\alpha$ (V/K)	$\rho$ ( $\Omega$ mm)	$\kappa$ (W/m-K)	$C'''$ (\$/mm <sup>3</sup> )	$C''$ (\$/mm <sup>2</sup> )	Notes
Bi <sub>2</sub> Te <sub>3</sub> -Sb <sub>2</sub> Te <sub>3</sub>	Alloy	0.0001585	0.1621645	0.24	0.000865743;	0.00000476	[27]
PEDOT:PSS	Polymer	0.00021	0.135135135	0.37	0.00000051	0.00000476	[9]